What happens to polymer chains confined in rigid cylindrical inorganic (AAO) nanopores

Laurence Noirez, C. Stillings, J.-F. Bardeau, M. Steinhart, S. Schlitt, J. H. Wendorff, G Pépy

Macromolecules

Article

pubs.acs.org/Macromolecules

What Happens to Polymer Chains Confined in Rigid Cylindrical Inorganic (AAO) Nanopores

L. Noirez,*[,†] C. Stillings,[§] J.-F. Bardeau,[⊥] M. Steinhart,[∥] S. Schlitt,[§] J. H. Wendorff,[§] and G. Pépy[‡]

[†]Laboratoire Léon Brillouin (CEA-CNRS), CE-Saclay, 91191 Gif-sur-Yvette Cédex, France

[‡]Research Institute for Solid State Physics and Optics, 1525 Budapest, Pf. 49. Hungary

[§]Fachbereich Chemie, Philipps-Universität Marburg, D-35032 Marburg, Germany

[⊥]Institut des Molécules et Matériaux du Mans, UMR CNRS 6283, Université du Maine, Avenue Olivier Messiaen, 72085 Le Mans, France

[∥]Institut für Chemie neuer Materialien, Universität Osnabrück, Barbarastrasse 7, D-49069, Osnabrück, Germany

ABSTRACT: Nanoconfinement can profoundly change the bulk characteristics. The question of conformational changes under one-dimensional confinement is recurrent in polymer physics. Very few works addresses this question because of the hard experimental challenge and the complex analysis of the signal. Here, the conformation of polystyrene chains shaped by wetting, in nanotubes or nanorods is for the first time determined at 3 dimensions. Polystyrene chains (molecular weight samples from 38 kDa to 310 kDa) confined in AAO nanopores as large as the size of the pore diameters (from 35 to 180 nm) are probed, revealing the invariance with respect to the bulk-like conformation for polystyrene chains up to 301 kDa confined down to 35 nm diameter nanopores.

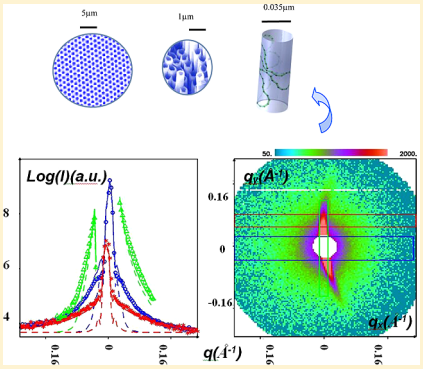

1. INTRODUCTION

One-dimensional nanomaterials such as nanowires and nanotubes will assume increasingly significant proportions.[1,2] Their unique properties are appropriated to a wide choice of materials[1−6] and to various applications as displays and magnetic media,[7] separation of racemic mixtures,[8] selective ion transport[9] or sensors.[10] Martin et al. have pioneered a versatile and efficient methodology using high surface energy matrices as molds.[6,11] The high surface energy improves the wetting and thus the filling of the nanopores to prepare such 1D nanoobjects. Anodic aluminum oxide (AAO) templates[12−14] are characterized by hexagonally arranged, parallel pores with defined diameter distribution a high aspect ratios and uniform pore depth.[5,6] Nanowire arrays prepared with AAO as a mold, exhibit high regularity and high orientation over centimeter length scales. The question of how 1D-geometric confinement and the nature of the pore walls influence the morphology of the "molded" material, particularly in case of mesoscopic length scale systems as polymers, is debated and remains largely unanswered. Experimental methods as surface force apparatus, Brillouin scattering, calorimetry, point out deviation from polymer bulk properties,[15] sometimes impressive: a decrease of about 60 °C with respect to the bulk glass transition temperature is observed in freestanding film.[16] In contrast, few studies aim at relating these changes to dimensional parameters. Ideally, the polymers close to the inner pore surface might exhibit either brush-like layers for a high density of chains per surface unit, or flat coils with few contact points to the surface. In both cases, a deviation from the isotropic statistic chain is expected. The very first works dealing with the determination of the polymer shape in restricted geometry have been reported by Russell et al.[17,18] They searched deviation from bulk dimensions on ultrathin films of polystyrene[17] and on polystyrene chains filling AAO nanopores. While no change was observed on ultrathin films, a chain contraction perpendicular to the nanopore axis[18] was deduced from small-angle neutron scattering (SANS) data. In another neutron scattering study,[19] no apparent form factor anisotropy was detected on polyethylene oxide chains (POE) whose signal was modeled as a one-dimensional Debye function. The present study reports on a complete SANS study analyzing for the first time, in three dimensions, the conformation of polystyrene chains confined in AAO membranes.

When molten polymers are in contact with the wetting nanopore, an inner mesoscopic film is formed.[20] At an early stage, the wetting produces polymer nanotubes of typically hundred micrometers long and 10−30 nm thick. The nanotube process is favored by low molecular weights while nanorods are mostly observed with large molecular weights. In the present letter, the chain conformation in both nanotube and nanorod confined geometry are examined, the filling state being

Received: March 15, 2013
Revised: May 13, 2013
Published: June 6, 2013

   dx.doi.org/10.1021/ma4005605 | *Macromolecules* 2013, 46, 4932−4936

characterized by atomic force microscopy.[21] The determination of average size and shape of the chain is obtained by small-angle neutron scattering (SANS) using a specific labeling of the polymer chains. The study is carried out at room temperature, on a series of different molecular weight polystyrenes shaped in AAO membranes of 35 and 180 nm pore diameters. Four molecular weights are chosen to display chain radii of gyration (R_g = 5.4, 7.9, 8.4, 15.6 nm respectively) comparable to the mesoscopic film thickness and comparable to the smaller nanopore diameter (35 nm) for the higher molecular weight ($2R_g$ = 31 nm). We analyze both the influence of the molecular weight and of the template matrix diameter on the chain conformation and compare the results to the bulk dimensions.[22]

2. EXPERIMENTAL SECTION

Hydrogenated (PS) and deuterated (dPS) polystyrene (d8) were purchased from Polymer Source. The averaged weight-average molecular weights of the PS/dPS midxture are $\langle M_w \rangle_{PS/dPS}$ = 38 kDa, 80 kDa, 91 kDa, and 301 kDa with polydispersity indices smaller than 1.2.

Isotopic mixtures of PS and dPS were necessary to create the scattering contrast to visualize the chain form factor by SANS.[23] PS and dPS were mixed in 1:1 proportion, by dissolution in dichloromethane, precipitation in methanol and dried in a vacuum. Self-ordered AAO with a pore diameter of 35 nm and a lattice constant of ~100 nm as well as AAO with a pore diameter of 180 nm and lattice constant of 500 nm was prepared by the two-step anodization.[12,13] The pore depth (thickness of AAO layer) was adjusted to 100 μm. The PS/dPS mixtures with M_w = 38 kDa, M_w = 91 kDa were placed on AAO membranes heated to 200 °C under argon. The samples were kept at 200 °C for 10 min and slowly cooled to room temperature under vacuum. The PS/dPS mixture with M_w = 301 kDa was placed on AAO membranes heated to 220 °C under argon. The samples were kept at 200 °C for 10 h and slowly cooled to room temperature under vacuum. Excess polymer was removed from the AAO surfaces with sharp blades and by treatment with oxygen plasma for 7 min at 100 W and 0.9 mbar (Technis Plasma Processor 100E Tepla 100).

AFM measurements have been carried out in intermittent contact-mode with an Agilent 5500 AFM using no Contact Focused Electron Beam (FEB) "whisker type" (NSCO5_10°, NT-MDT) tips. Samples of lower molecular weight (M_w = 37600 g/mol) present opened tubes, indicating that the walls of the AAO membrane have been wetted (nanotubes) while higher molecular weights ($M_w \geq$ 91000 g/mol) exhibit closed hexagonal nanopillar arrays in agreement with the geometry and the size of AAO pores and a filling (nanorods).

SANS experiments have been carried out with the position sensitive neutron detector PAXY of the Laboratoire Léon Brillouin.

3. MEMBRANE SCATTERING AND MODELING

The polymer nanotubes were kept in the native AAO membranes for an easy positioning with respect to the scattering geometry. Figure 1 illustrates the scattering geometry with the pore axe in the horizontal plane and close to the neutron trajectory (vertical membrane configuration).

The scattering combines the contribution of the form factor of the polymer chains scaling as q^{-2} (in the Guinier domain) and a sharp anisotropic signal observable on both filled and empty membranes.[24,25] The strong anisotropic signal can originate from different interfacial scattering (cavity of the tube and the AAO membrane (empty template), cavity of the nanotube and polymer nanotube, polymer and AAO membrane). The persistence of the strong anisotropic signal whatever the sample orientation points out that it is nearly impossible to avoid it. Similarly, a contrast matching is hardly applicable since different and strong interfacial scattering of

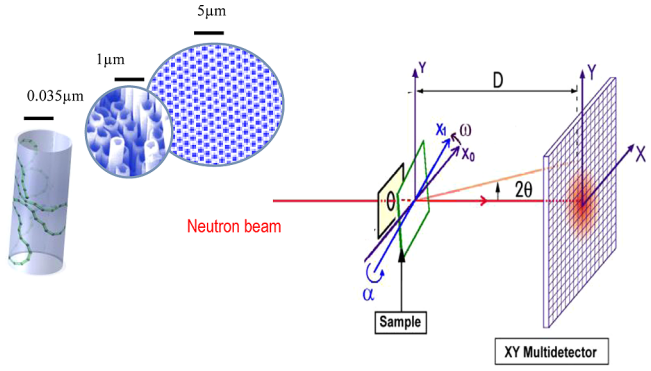

Figure 1. Setup: The AAO membrane (green rectangle) is placed vertically in front of the incident beam (vertical configuration). The pore axes are perpendicular to the plane of the AAO membrane. To limit the membrane scattering and access the direction transverse to the nanotube axis, the AAO plane is rotated of an angle α around the horizontal axis X_0, and of an angle ω around the vertical axis (Y). In the "horizontal" configuration, the AAO plane is nearly horizontal (ω is close to 0° and α is large but not 90° since the sample cross-section would be polluted by multiple scattering). The inset shows a photograph of the porous AAO membrane and of polymer nanotubes.

different coherent scattering lengths (AAO nanopore interface versus polymer, polymer/air interface) have to be matched simultaneously. Therefore, we adopt a strategy consisting in optimizing the chain signal (using a 1:1 isotopic mixture of PS/dPS) and analyzing all scattering contributions without matching. The interfacial scattering being the strongest contribution will be first modeled, followed by an analysis of coupling terms, and finally of the 3D polymer form factor.

The Fourier transform of a (filled or unfilled) straight cylinder is

$$S(q) = 2KJ_1(q_\perp R)/(q_\perp R)\,\sin(q_z L)/q_z L \qquad (1)$$

where K is the difference between the neutron scattering lengths inside and outside the channel, J_1 is a Bessel function, $Q_\perp$ and Q_z the scattering vector components perpendicular and along the channel axis, and L and R are the nanotube half length and the nanotube radius, respectively.[25] To test this model without contribution of the chain form factor, empty AAO or AAO containing hydrogenated PS are first used. At small scattering vectors (0.003 < Q < 0.02 Å^{-1}), the signal exhibited by 35 nm diameter AAO membrane is more complex than a straight cylinder function (Figure 2). It is modulated by the structure factor of the hexagonal ordering. This modulation is neither observed on larger nanopores (typically on 180 and 400 nm nanopore diameters) nor at large scattering vectors.

The oscillations decrease very fast with the scattering angle and are no more visible for q > 0.02 Å^{-1}. This is due to the large aspect ratio (channel length/diameter, $2L/R$). In the range of observation for the polymer chain conformation (Guinier range), the apparent absence of oscillations at larger scattering vectors allows the use of a simplified model of the straight cylinder. In eq 1, the radial term $J_1(q_rR)/(q_rR)$ is approximated to a Porod scattering $(q_rR)^{-3}$. The longitudinal term, $\sin(q_zL)/q_zL$, is kept with a 10% dispersion over L to smooth out the "longitudinal" oscillations.

Figure 3 displays the scattering obtained in the scattering range 0.02 < q < 0.2 Å^{-1}, on vertically oriented AAO pore of 180 nm average diameter containing protonated PS. The left panel shows the 2D fit of the scattering modeled with the

dx.doi.org/10.1021/ma4005605 | Macromolecules 2013, 46, 4932−4936

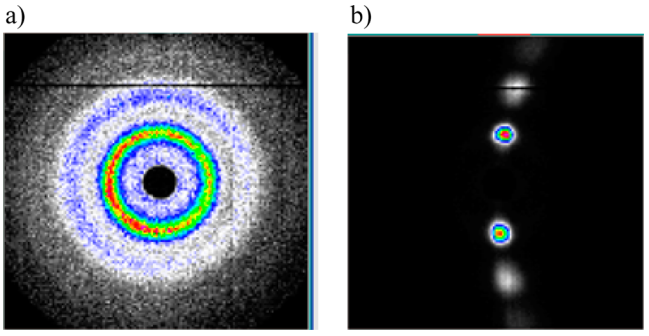

Figure 2. Typical modulated signal produced by the AAO membrane (35 nm diameter) oriented with the nanotubes nearly parallel to the incident beam observed at very small scattering vectors (D = 6.7 m, λ = 14 Å). (a) The centrosymmetric scattering rings overwhelm any other signal and do not enable the access to a polymer scattering. (b) AAO membrane is tilted from 6° about the vertical axis with respect to Figure 3a in order that the AAO signal intercepts the Ewald sphere in a narrow crescent.

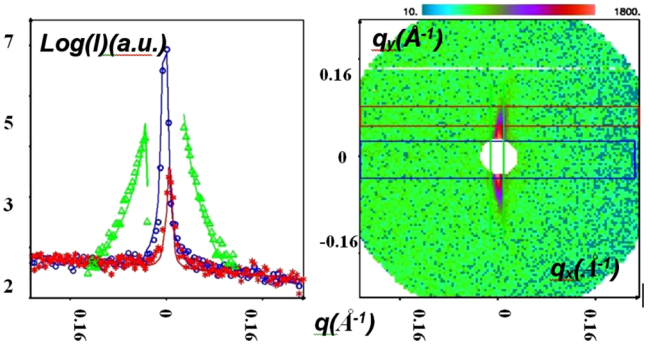

Figure 3. Modeling of the 2D neutron scattering produced by a 180 nm diameter AAO membrane filled with a 38 kDa protonated polymer (vertical membrane configuration). The left panel displays the experimental data along the areas defined by rectangles of the same color in the 2D pattern (right figure) and the fit by a simplified cylinder model (continuous lines). The green data correspond to the vertical direction, whereas blue and red data represent the two horizontal areas. Scattering conditions: D = 1.5 m; λ = 5.5 Å. Similar scattering is obtained without polymer or with other molecular weights.

simplified straight cylinder model. The fitting program is the PXY7 2D data treatment software.[26] The model is in agreement with the foren values. A perfect agreement is however difficult to obtain since the model is approximated and in case of extreme anisotropic signals, small variations in the input data produce large discrepancies.

4. EXTRACTING POLYMER CONFORMATION FROM THE NANOTUBE SIGNAL

To access the polymer form factor,[23] we analyze the signal of the AAO membranes filled with the 1:1 PS/dPS mixture. The chain dimensions are determined in the Guinier regime using the full form factor expression:

$$I(q) = \frac{I_0}{1 + q_x^2 R_x^2 + q_y^2 R_y^2 + q_z^2 R_z^2} \quad (2)$$

where q is the scattering vector and R_z and R_x, R_y, the components of the radius of gyration R_g, along (R_z) and perpendicular ($R_x = R_y$) to the AAO pore axis, respectively ($R_g^2 = R_x^2 + R_y^2 + R_z^2$).

In order to access the three components of the radius of gyration, the "horizontal" and the "vertical" template configurations were used. Tilting the AAO membrane (Figure 3b) concentrates the signal from the AAO pore along an axis, allowing access to the polymer form factor in the rest of the reciprocal space.

The polymer form factor is first determined from the scattering area not affected by the AAO scattering. AAO pore scattering is discriminable from polymer scattering since it is strongly sensitive to a weak sample rotation contrarily to the polymer signal. After several trials, the pixels whose scattering differed by more than 2.5 mean square deviations when rotating the sample by about 10° about the vertical axis, were considered as being contaminated by the nanopore scattering.

The horizontal orientation of the AAO membrane offers an ideal configuration to access to an eventual anisotropy of the polymer form factor. In this geometry, the nanotubes within the (horizontal) plane of the AAO membrane, are oriented (vertically) nearly perpendicular to the incident beam. The AAO scattering being extremely extended along the horizontal axis as seen on Figure 4, is excluded from the treatment zone, enabling the analysis of the polymer form factor along and perpendicular to the AAO pore axis.

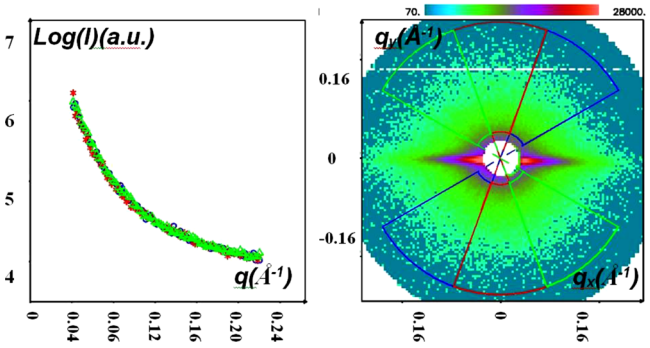

Figure 4. Invariance of the radial neutron scattering profiles along different sectors (blue line, 30−70°; red line, 70−110°; green line, 110−150°) indicating the isotropic distribution of the chains along and transverse to the AAO axis. Sample: 35 nm diameter AAO nanopore filled with a 38 kDa PS/dPS mixture−horizontal membrane configuration.

While direct access to the longitudinal chain scattering is excluded, no change of the scattering shape is observed from transverse sectors to sectors close to the longitudinal direction. The scattering invariance (superposition of the scattering in the different sectors—Figure 4) shows a similar scattering along the transverse and longitudinal directions. The modeling fits with the form factor of the polymer chain in the bulk (see Table 1). The same observation is done for all samples, irrespective of pore diameter and molecular weight (Figure 5). Therefore, it can be concluded first that there is no need to add of coupled term due to the interference between the AAO pore scattering and the polymer form factor. Second, the chains forming the nanotubes are not affected by surface or confinement effects, and exhibit bulk-like isotropic conformations.

Finally, we test the validity of the superposition of the AAO pore signal by the straight cylinder model and the chain form factor signal by the Lorentzian, by simultaneously fitting both

dx.doi.org/10.1021/ma4005605 | Macromolecules 2013, 46, 4932−4936

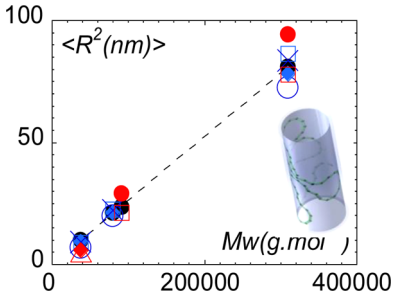

Figure 5. Chain dimensions versus AAO pore diameter (the square of the chain dimensions is preferred since $\langle R^2 \rangle$ scales with M_w)). (·) R_i(bulk). The blue symbols correspond to the component of the radius of gyration in 180 nm diameter nanotubes and the red ones to components in 35 nm diameter. Key: blue □, R_x(180 nm); blue ○, R_x(180 nm); blue ×, R_z(180 nm); red △, R_x(35 nm); red ◆, R_x(35 nm); red □, R_x(35 nm); red ●, R_z(35 nm).

signals. Figure 6 displays an example of simultaneous treatment of this complex scattering.

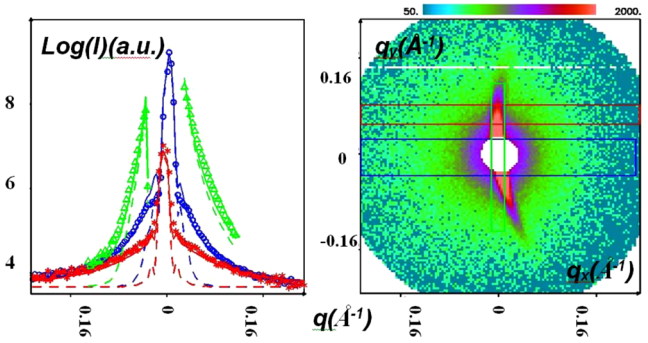

Figure 6. Highlight of the coherence between experimental data (180 nm pore diameter AAO membrane filled with a 80 kDa PS/dPS mixture−vertical membrane configuration) and modeling. The left figure displays the intensity and the fit following the vertical direction (green data), whereas blue and red data describe two selected horizontal zones. The dotted lines represent the cylinder form factor alone.

The relative adequacy of the model to the experimental data shows that the preliminary analysis of the complex signal produced by nanopores filled with nanocylinder polymer fits with the superposition of a cylinder form factor and a conventional polymer form factor. This agreement evidence that these two signals are not coupled and confirms the relevance of modeling the strong nanotube scattering using a simplified straight cylinder model.

5. CONCLUSIONS

The 3-dimensional description of the conformation adopted by a polymer chain shaped in nanotubes or in nanorods in cylindral AAO nanopores is for the first time directly determined. The complex SANS signal produced by nanopores infiltrated with polystyrene is successfully modeled by the superposition of a simplified straight cylinder form factor and a conventional polymer form factor. The analysis of the polymer form factor shows that the chain extension is similar along the transverse and longitudinal direction to the AAO axes. It can be concluded that the polystyrene chain remains isotropic in both configurations when a thin polymer layer wets the AAO nanopore or when it fills pore diameters as large as the size of the polymer (twice its radius of gyration). Even though the confinement could be considered as moderate, the absence of chain anisotropy in this configuration reveals that the interactions with the other chains or the interchain with the walls play no role in the polymer entropy. It seems that the process of formation of nanocylinders via a mesoscopic film (wetting process) does not modify the molecular entropic equilibrium from its early stage (opened nanotube) to the final stage (filled nanorod). This result contrasts with observations carried out on spin-coated polystyrene films that show an extension of the quenched chains on the surface,[27] or a structuration down to the substrate.[28] The later are probably relevant of a nonequilibrium state. In contrast, the nanofabrication of polymer tubes via a mesoscopic film keeps unchanged the chain shape. The present high accuracy results enable to exclude a chain contraction perpendicular the nanopore axis as announced in a previous analysis[18] on the basis of an incomplete neutron scattering experiments. We assume that the findings are generic to all nanocomposites shaped by wetting contact.

AUTHOR INFORMATION

Corresponding Author

*E-mail: (L.N.) laurence.noirez@cea.fr.

Notes

The authors declare no competing financial interest.

REFERENCES

(1) Martin, C. R. *Science* **1994**, *266*, 1961.
(2) Huang, Y.; Duan, X. F.; Cui, Y.; Lauhon, L. J.; Kim, K. M.; Lieber, C. M. *Science* **2001**, *294*, 1313.
(3) Schnur, J. M. *Science* **1993**, *262*, 1669.
(4) Evans, E.; Bowman, H.; Leung, A.; Needham, D.; Tirrell, D. *Science* **1996**, *273*, 933.
(5) Bognitzki, M.; Hou, H. Q.; Ishaque, M.; Frese, T.; Hellwig, M.; Schwarte, C.; Schaper, A.; Wendorff, J. H.; Greiner, A. *Adv. Mater.* **2000**, *12*, 637.
(6) Steinhart, M.; Wendorff, J. H.; Greiner, A.; Wehrspohn, R. B.; Nielsch, K.; Schilling, J.; Choi, J.; Gösele, U. *Science* **2002**, *296*, 1997.
(7) Kovtyukhova, N. I.; Mallouk, T. E.; Mayer, T. S. *Adv. Mater.* **2003**, *15*, 780.
(8) Lee, S. B.; Mitchell, D. T.; Trofin, L.; Nevanen, T. K.; Soderlund, H.; Martin, C. R. *Science* **2002**, *296*, 2198.
(9) Nishizawa, M.; Menon, V. P.; Martin, C. R. *Science* **1995**, *268*, 700.
(10) Steinle, E. D.; Mitchell, D. T.; Wirtz, M.; Lee, S. B.; Young, V. Y.; Martin, C. R. *Anal. Chem.* **2002**, *74*, 2416.
(11) (a) Steinhart, M.; Wendorff, J. H.; Wehrspohn, R. B. *Chem. Phys .Chem.* **2003**, *4*, 1171. (b) Steinhart, M.; Wehrspohn, R. B.; Gösele, U.; Wendorff, J. H. *Angew. Chem., Int. Ed.* **2004**, *43*, 1334.
(12) Masuda, H.; Fukuda, K. *Science* **1995**, *268*, 1466.
(13) Masuda, H.; Yada, K.; Osaka, A. *Jpn. J. Appl. Phys., Part 2* **1998**, *37*, L1340.
(14) Nielsch, K.; Choi, J.; Schwirn, K.; Wehrspohn, R. B.; Gösele, U. *Nano Lett.* **2002**, *2*, 677.
(15) Inoue, R.; Kawashima, K.; Matsui, N.; Nakamura, K.; Nishida, K.; Yamada, N. L. *Phys. Rev. E* **2011**, *84* (031802), 1.
(16) Forrest, J. A.; Dalnoki-Veress, K.; Stevens, J. R.; Dutcher, J. R. *Phys. Rev. Lett.* **1996**, *77*, 2002.
(17) Jones, R. L.; Kumar, S. K.; Ho, D. L.; Briber, D. L.; Russell, T. *Nature* **1999**, *400*, 146.
(18) Shin, K.; Obukhov, S.; Chen, J. T.; Huh, J.; Hwang, Y.; Mok, S.; Dobriyal, P.; Thiyagarajan; Russell, T. *Nat. Mater.* **2007**, *6*, 961.
(19) Martin, J.; Krutyevar, M.; Monkenbusch, M.; Arbe, A.; Allgaier, J.; Radulescu, A.; Falus, P.; Maiz, J.; Mijangos, C.; Colmenero, J.; Richter, D. *Phys. Rev. Lett.* **2010**, *104*, 197801.

(20) Léger, L.; Erman, M.; Guinet-Picard, A. M.; Ausserre, D.; Strazielle, C. *Phys. Rev. Lett.* **1988**, *60*, 2390.
(21) Binning, G.; Quate, C. F.; Gerber, Ch. *Phys. Rev. Lett.* **1986**, *56*, 930.
(22) Pedersen, J. V.; Schurtenberger, P. *Macromolecules* **1996**, *29*, 7602.
(23) (a) de Gennes, P. G. *Scaling Concepts in Polymers*; Cornell University Press: Ithaca, NY, 1979. (b) Cotton, J. P.; Decker, D.; Benoit, H.; Farnoux, B.; Higgins, J.; Jannink, G.; des Cloizeaux, J.; Ober, R.; Picot, C. *Macromolecules* **1974**, *7*, 863.
(24) Pépy, G.; Kuklin, A. *Nuc. Instrum. Methods B* **2001**, *185*, 198.
(25) Pépy, G.; Boesecke, P.; Kuklin, A.; Manceau, E.; Schiedt, B.; Siwy, S.; Toutemonde, M.; Trautmann, C. *J. Appl. Crystallogr.* **2007**, *40*, s388.
(26) G. Pépy, G. *J. Appl. Crystallogr.* **2007**, *40*, s433.
(27) Brulet, A.; Boué, F.; Menelle, A.; Cotton, J. P. *Macromolecules* **2000**, *33*, 997.
(28) Mudkhopadhyay, M. K.; Jioa, X.; Lurio, L. B.; Jiang, Z.; Stark, J.; Sprung, M.; Narayanan, S.; Sandy, A. R.; Sinha, S. K. *Phys. Rev. Lett.* **2008**, *101*, 115501.